

Cartilage Specific MR Sequences in Assessment of Lunate Types and Their Impact on Triangular Fibrocartilage

Kıkırdağa Özgün MR Sekansları ile Lunat Tipleri ve Bunların Triangüler Fibrokartilaja Etkisinin Değerlendirilmesi

© Zehra Akkaya¹, © Elif Peker¹, © Başak Gülpınar¹, © Ayşegül Gürsoy Çoruh¹, © Sena Ünal¹, © Mehmet Mesut Çelebi², © Gülden Şahin¹

¹Ankara University Faculty of Medicine, Department of Radiology, Ankara, Turkey

²Ankara University Faculty of Medicine, Department of Sports Medicine, Ankara, Turkey

Abstract

Objectives: Our purpose was to investigate the effects of different lunate morphologies on triangular fibrocartilage (TFC) using cartilage specific magnetic resonance imaging (MRI) sequences. Secondly, we aimed to define better parameters to discriminate two lunate types on MRI and posteroanterior wrist radiographs.

Materials and Methods: Wrist MRIs of 118 cases with neutral ulnar variance were retrospectively assessed for lunate types based on the presence of abutting articular cartilage between lunate and hamate on coronal 3D dual echo steady state and 2D multi-echo data image combination images. Posteroanterior radiographs were assessed separately. TFC and cartilage lesions on hamate and lunate were assessed on MRI. Lunate-hamate (L-H) and capitate-triquetrum (C-T) distances were measured on coronal MRI and radiographs. Relationship between lunate types and cartilage lesions were evaluated using X², Fisher's exact test, t-test or Mann-Whitney U test. ROC analysis was used to determine cut-off values to best discriminate the two lunate types.

Results: Mean age was 38.5±13.4 (M:F=33:85). TFC or lunate cartilage lesions showed no correlation with lunate types. L-H/C-T ratio of 0.907 on MRI and 0.75 on radiographs yielded the highest sensitivity and specificity for discrimination of lunate types. Type 2 morphology was correlated with cartilage degeneration on hamate (p=0.003). Cartilage lesions on hamate, lunate and TFC were significantly correlated with age (p=0.008, p=0.003, p<0.001 respectively).

Conclusion: Lunate types had no impact on degenerative changes of TFC or lunate-sided cartilage damage in wrists with neutral ulnar variance, however type 2 morphology was highly correlated with hamate-cartilage degeneration. Age was correlated with degenerative findings on all cartilage surfaces.

Key Words: Hamatolunate Impingement, Lunate Morphology, MRI, Radiographs, Wrist

Öz

Amaç: Amacımız, kıkırdağa özgün manyetik rezonans görüntüleme (MRG) sekansları kullanarak değişik lunat morfolojilerinin triangüler fibrokartilaj (TFK) üzerindeki etkilerini araştırmaktır. İkincil olarak MRG ve posteroanterior el bilek grafilerinde lunat tiplerini ayırmada daha iyi parametreler tanımlamayı amaçladık.

Gereç ve Yöntem: Koronal 3B dual echo steady state ve 2D multi-echo data image combination MR görüntüleri kullanılarak 118 nötral varyanslı el bileği MR incelemesinde lunat ve hamat kemiklerin karşılıklı temas eden kıkırdağ yüzeyi olup olmasına göre lunat tiplendirmesi yapıldı. Ayrı

Address for Correspondence/Yazışma Adresi: Zehra Akkaya

Ankara University Faculty of Medicine, İbni Sina Hospital, Clinic of Radiology, Ankara, Turkey

E-mail: zehraakkaya@gmail.com ORCID ID: orcid.org/0000-0002-6483-3381

Received/Geliş Tarihi: 05.05.2021 Accepted/Kabul Tarihi: 09.01.2023

*This study was presented as an oral presentation in the annual meeting of Turkish MRI Society in 2018 in Ankara and a short abstract of this study was published in May 2018 as Supplement 1 of Eurasian Journal of Medicine (Eurasian J Med 2018; 50: Supplement 1-45 DOI: 10.5152/eurasianjmed.2018.02052018).

©Copyright 2022 Ankara University Faculty of Medicine

Journal of Ankara University Faculty of Medicine is published by Galenos Publishing House.

All content are under CC BY-NC-ND license.



bir seansta posteroanterior el bilek grafilerinde lunat tipleri değerlendirildi. MRG'de TFK, hamat ve lunat eklem kıkırdak lezyonları değerlendirildi. Koronal MRG ve grafilerden lunat-hamat (L-H) ve kapitat-trikuetrum (K-T) mesafeleri ölçüldü. Lunat tipleri ile kıkırdak lezyonları arasındaki ilişkinin değerlendirilmesinde X2, Fisher's exact test, t-test veya Mann-Whitney U testleri kullanıldı. İki lunat tipini ayırmada en iyi eşik değeri tespit etmede ROC eğrisi analizi kullanıldı.

Bulgular: Ortalama yaş $38,5 \pm 13,4$ (E:K=33:85) idi. TFC ve lunat kıkırdak lezyonları ile lunat tipleri arasında ilişki saptanmadı. MR'de L-H/K-T MR için 0,907, direct grafilerde 0,75 lunat tiplerini ayırmada en yüksek duyarlılık ve özgüllüğü gösterdi. Tip 2 morfoloji hamatta kıkırdak dejenerasyonu ile korele bulundu ($p=0,003$). Yaş, hamat, lunat ve TFC kıkırdak lezyonları ile ilişkili bulundu (sırasıyla $p=0,008$, $p=0,003$, $p<0,001$).

Sonuç: Nötral varyanslı el bileklerinde lunat tiplerinin TFC ve lunat kıkırdak üzerinde etkisi gözlenmezken tip 2 lunat morfolojisi hamat kıkırdak dejenerasyonu ile korele bulundu. Yaş, her üç kıkırdak yüzeydeki dejeneratif değişiklikler ile koreleydi.

Anahtar Kelimeler: Hamatolunat Sıkışma, Lunat Morfolojisi, MRG, Direkt Grafi, El Bileği

Introduction

Lunate, with its central position in the proximal carpal row, is subjected to substantial axial and torsional forces during flexion-extension, ulnar and radial deviation and pronation-supination of the wrist (1). Anatomically it is classified into two types based on its relationship to hamate. A type 1 lunate has a single distal articular facet for capitate, whereas a type 2 lunate has an additional medial (ulnar) facet articulating with hamate (2,3). A type 2 lunate with a reported rate of 44-73% in various studies (4-9) has been shown to significantly influence the vascular pattern, ligamentous anatomy, load bearing characteristics and kinematic of carpal bones (2,3,6,9-11). Subsequently, it has been shown that the two variant shapes of lunate are associated with differences in progression and development of several wrist disorders, including hamatolunate impingement (12-14), Kienböck's disease (11,15,16), scapho-trapezio-trapezium joint degeneration (17), progression to non-union following scaphoid fractures and dorsal intercalated segment instability deformity (18-20). Hamatolunate impingement syndrome is a cause of ulnar sided wrist pain, characterized by degenerative changes at the opposing facets of dorsal and central aspect of proximal pole of hamate and lunate particularly with a medial lunate facet width of 3 mm or wider (6,7,12). Moreover, components of triangular fibrocartilage complex (TFCC), which together with lunotriquetral ligament, play a key role in stabilizing lunate, make up another important and well-documented cause of ulnar sided wrist pain when damaged. The anatomical position of the central disc of TFCC (TFC) immediately proximal to lunate, may render it to various shearing forces and stress during wrist motions, particularly during ulnar deviation. Despite the intricate anatomical relationship and similar clinical findings of hamatolunate impingement and ulnar impaction syndromes, there are only few studies which evaluate the direct influence of lunate morphology on ulnocarpal joint in detail (8,21).

Several MRI and magnetic resonance arthrography studies, correlated with cadaveric dissections have demonstrated

that using MR techniques, lunate morphology and chondral changes at hamatolunate junction can be readily outlined (4,7,8). Especially with the use of higher field strength magnets and multichannel phase array coils, better spatial resolution and signal to noise ratios are achieved making MRI an excellent tool for assessment of wrist (22,23). However, in clinical practice, due to their wide availability, radiographs remain to be the first choice of imaging study for evaluation of various wrist disorders. With an accuracy of 66 % for detection of type 2 lunate, radiographs are far from ideal in morphologic assessment of lunate types, thereby detection of wrists at risk for midcarpal joint degeneration (24). Despite the recognition of clinical and radiological findings and significant implications of type 2 lunate, better criteria are needed to assess the lunate morphology on radiographs.

The main purpose of this study was to evaluate the effects of lunate type on the degenerative changes of TFC. Secondly we sought to define more objective and reproducible methods of assessing lunate type on imaging studies.

Materials and Methods

Ethics committee approval (Approval no: 10-789-19, Date: 27.05.2019) was obtained for this study from the Ankara University Faculty of Medicine Ethics Committee and patient informed consent was waived.

Study Population

Patients between the ages 18 and 65, who had a 3.0 T MRI of the wrist between July 2011 and March 2018 were included in this retrospective study.

Patients with positive or negative ulnar variance on posteroanterior (PA) radiographs, history of wrist surgery, congenital or acquired wrist deformity, inflammatory arthritides, carpal coalition were excluded. Additionally, patients whose MRI scans did not include a 3D dual echo steady state (3D-DESS) sequence, patients who did not have a PA radiograph obtained within six months from the MRI scan, or patients with technically inadequate imaging studies (motion artefacts on MRI, positioning errors on radiographs) were also excluded.

Image Acquisition

All patients were scanned with a 3.0T scanner (Siemens Magnetom Verio, Erlangen Germany) in prone position with their arm extended above the head and hand in pronation ("superman" position) and in isocenter of the scanner, using an 8-channelled coil. The wrist MRI protocol included, coronal and axial fast spin echo (FSE) T1-weighted images (TR/TE: 677-400/20-13 ms, averages: 3, bandwidth: 130 kHz, matrix: 384x242-320x256, FOV: 120x120 mm, interslice gap: 0.3 mm), coronal short tau inversion recovery images (TR/TE: 4000/42 ms, TI: 200 ms, averages: 1, bandwidth: 203 kHz, matrix: 256x230, FOV: 120x120 mm, slice thickness: 3 mm, interslice gap: 0.3 mm) coronal fat saturated intermediate weighted (fs-IW) images (TR/TE: 3130/35 ms, averages: 1, bandwidth: 181 kHz, matrix: 256x218, flip angle: 150°, FOV: 120x120 mm, slice thickness: 3 mm, interslice gap: 0.3 mm), sagittal fs-FSE T2-weighted sequence (TR/TE: 3800/69 ms, average: 3, bandwidth: 230 kHz, matrix: 256x192, FOV: 120x120 mm, slice thickness: 3.5 mm, interslice gap: 0.4 mm), T2-W 3D-DESS images (T2-de3d) (TR/TE: 13.4/5.2 ms, matrix: 220x256, FOV: 160x160 mm, NEX: 1, number of slices: 112, slice thickness: 0.8 mm, interslice gap: 0 mm, flip angle: 30° bandwidth: 283 kHz, matrix: 256x192), 2D-T2-W multi-echo data image combination (MEDIC) images (TR/TE: 687/22 ms, slice thickness: 3 mm, interslice gap: 0.3 mm, flip angle: 20, Averages: 1, FOV: 120x120 mm, bandwidth: 250 kHz, matrix: 256x192).

Standard PA radiographs of the wrist were evaluated. When serial radiographs were available, the one with the shortest time interval until the MR scan was used.

Image Analysis

Two musculoskeletal radiologists, one with 5 years of experience (ZA) and the other with more than 20 years of experience (GS) reviewed all the MR images in consensus for lunate morphology, cartilage and subchondral bone changes at opposing facets of lunate and hamate and pathologic changes in TFC.

The lunate types were assessed based on the presence or absence of reciprocal opposing cartilage surfaces on distal lunate and proximal hamate, especially on the dorsal-most aspect of the midcarpal joint on 3D-DESS and T2W-MEDIC images. Cases with reciprocal articular cartilage surfaces in contact with each other were classified as type 2 (Figure 1a), cases in whom lunate and hamate articular cartilages were not in direct contact with each other were classified as type 1 lunate (Figure 1b) wrists.

TFC lesions were evaluated on a binary scale as normal or abnormal. The latter category included any TFC which demonstrated thinning, central defect or perforation with or without associated lunate and/or ulnar surface articular cartilage abnormality, findings of ulnocarpal joint arthrosis (osteophytes, subarticular erosions, sclerosis and cysts) (25).

Articular cartilage irregularity, subchondral cysts, subchondral bone marrow changes on hamatolunate joint facets and TFC lesions were assessed on all FSE sequences but coronal fs-IW images, 3D-DESS images and 2D-MEDIC images were most useful.

The 3D-DESS images were evaluated using multi-planar reconstruction technique when needed.

Two other radiologists with 15 years of experience in general radiology (EP, BG) reviewed PA radiographs in consensus blinded to MRI findings.

On radiographs, following the description of Pfirmann et al. (8) lunates with a distinguishable concave or straight medial facet for hamate bone were classified as type 2 lunates, and those without were classified as type 1 (Figure 2).

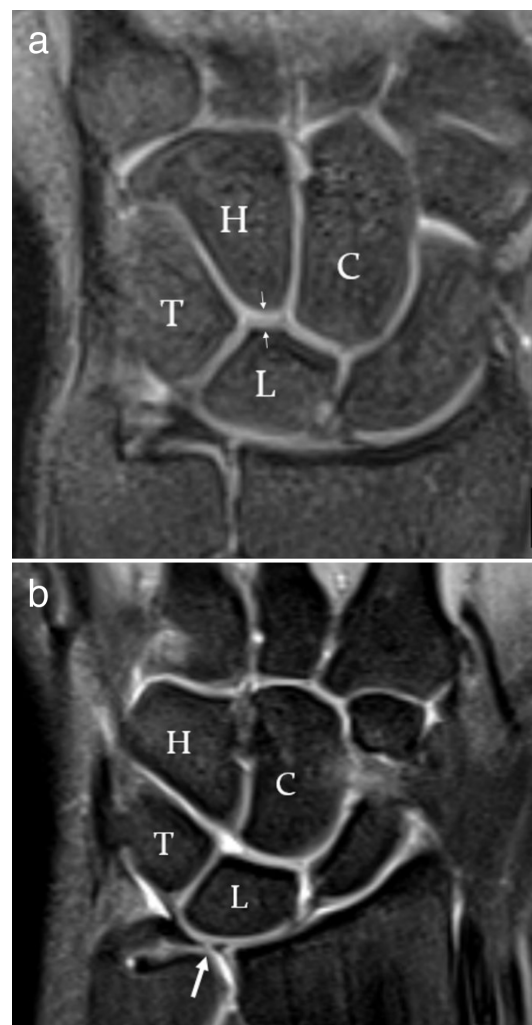


Figure 1: A coronal 3D- DESS image (a) of a patient with a type 2 lunate. Note the abutting articular cartilage surfaces (arrows) of hamate (H) and lunate (L). Coronal IW image (b) of a type 1 lunate wrist where lunate and hamate do not have abutting cartilage surfaces. Note the small perforation on the TFC (arrow)

C: Capitate, T: Triquetrum, TFC: Triangular fibrocartilage, IW: Intermediate weighted

Both group of observers measured the distances between lunate-hamate (H-L) and capitate-triquetrum (C-T) bony surfaces at the widest part of the hamate-lunate interface on coronal 3D-DESS images (Figure 3a, b) and radiographs (Figure 3c, d).

Statistical Analysis

Data was analysed using SPSS (Version 21.0, IBM Corp, Armonk, NY, USA). Continuous variables were given as means \pm standard deviation (range), categorical variables were given as frequencies (percentage). For comparison of categorical variables in two independent groups, chi-square and Fisher's exact tests, for continuous variables independent samples t-test and Mann-Whitney U test were used. Receiver operating characteristics (ROC) analysis was used to evaluate the prognostic performance of significant parameters. Based on the area under the curve analysis threshold indices for discrimination of the two types of lunate bone were assessed when applicable using Youden index (sensitivity+specificity-1). Using the ROC curve, optimal cut-off values were defined whereby the maximum combination of sensitivity and specificity was achieved for detection of a type 2 lunate. Pearson's correlation analysis was used to assess the



Figure 2: Posteroanterior radiographs of wrist in two different patients with type 1 (a) and type 2 (b) lunates are shown. Note the pointy tip of proximal pole of hamate in type 1 configuration (arrow in a) and the straight medial lunate facet (open arrow in b) in type 2 configuration, with a more rounded hamate tip

MRI and radiographic evaluations for lunate types. Statistical significance was set at $p < 0.05$.

Results

A total of 118 patients (33 males, 85 females) were included in the study. Mean age was 38.5 ± 13.4 (median: 35, range: 18-74). Type 1 lunate morphology was detected in 25.4% (n=30) and type 2 lunate morphology was detected in 74.6% (n=88) cases. Table 1 shows the frequencies of lunate types with respect to genders.

Articular surface changes on the proximal pole of hamate showed statistically significant correlation with age and type 2 lunate morphology ($p=0.008$, $p=0.003$ respectively). In 90.5% of patients with articular surface changes on hamate, type 2 lunate was present. Mean ages of patients with normal and pathologic cartilage changes on proximal pole of hamate were 36 ± 1.4 and 43 ± 2.2 respectively.

Articular surface changes on medial facet of lunate showed statistically significant correlation with age ($p=0.003$) but not with lunate types ($p=0.166$). Mean ages of patients with normal and pathologic changes on lunate cartilage were 36.1 ± 1.3 and 45.3 ± 2.6 respectively.

In 88 patients with type 2 lunate, a total of 38 cases (43.2%) presented cartilage irregularities (n=32, 36.4%) and subchondral cystic changes (n=6, 6.8%) of proximal pole of hamate. Cartilage irregularity (n=25, 28.4%) and subchondral cysts (n=1, 1.1%) were less common on the medial lunate facet.

The L-H, C-T distances and their ratios (L-H/C-T) significantly correlated with lunate types on both MRI and radiographs. Table 2 demonstrates the results of all measurements and their level of significance for discrimination of type 2 lunates.

There were no statistically significant associations between TFC lesions and lunate types ($p=0.935$); hamate, lunate articular surface changes ($p=0.084$, $p=0.055$ respectively) or C-T distances ($p=0.166$). Patients with pathologic TFC were significantly older than patients with normal TFC ($p < 0.001$).

For gender, no statistically significant correlations were found for lunate types ($p=0.11$); articular surface changes in hamate ($p=0.749$) or lunate ($p=0.437$); TFC lesions ($p=0.369$); H-L distance ($p=0.423$) or C-T distance ($p=0.205$). Age was

Table 1: Distribution and incidence of MRI-based lunate types with respect to gender

Lunate type	Females	Males	Total
Type 1	25 (21.2%)	5 (4.2%)	30 (25.4%)
Type 2	60 (50.8%)	28 (23.7%)	88 (74.6%)
Total	85 (72%)	33 (27.9%)	118 (100%)

MRI: Magnetic resonance imaging

also found to be unrelated to H-L and C-T distances ($p=0.12$, $p=0.453$ respectively).

Using a ROC analysis, optimal cut-off values were defined whereby the maximum combination of sensitivity and specificity was achieved. The results of ROC curve estimates for MRI and radiographic measurements of H-L, C-T distances and their respective ratios are summarized in Table 3. The highest sensitivity and specificity for discrimination of type 2 lunate was observed on MRI with a cut-off value of 0.907 for H-L/C-T distance ratio (95.5% sensitivity and 83.3% specificity). For radiographic measurements, H-L/C-T ratio of 0.75 had higher sensitivity and specificity (75% and 73.3% respectively) to discriminate type 2 lunates than H-L or C-T distances alone.

Hamate-sided cartilage degeneration was significantly correlated with type 2 lunate when H-L/C-T ratio of 0.907 was

used as a threshold to assess lunate types on MRI ($p=0.01$), however no such relationship was observed for radiographic threshold of 0.75 ($p=0.133$). In patients with type 2 lunate C-T distances on MRI did not show statistical correlation with neither hamate-sided nor lunate-sided articular cartilage damage ($p=0.41$, $p=0.603$ respectively).

Pearson's r for correlation between visual assessment of lunate types on MRI and radiographs was 0.048 ($p=0.607$). Using H-L/C-T ratios, MRI and radiographs showed a Pearson's $r=0.361$ ($p<0.001$).

Discussion

In this study, we found no correlations between TFC lesions and lunate types in patients with neutral ulnar variance. Cut-off

Table 2: Mean lunate-hamate, capitate-triquetrum distances, distance ratios and their level of significance in discriminating type 2 lunates on MRI and radiographs

	MRI			Radiographs		
	Type 1	Type 2	p-value	Type 1	Type 2	p-value
Mean L-H \pm SD (mm)	3.4 \pm 0.38	2 \pm 0.05	<0.001	3.3 \pm 0.09	2.7 \pm 0.08	<0.001
Mean C-T \pm SD (mm)	2.7 \pm 0.07	5 \pm 0.12	<0.001	3.4 \pm 0.1	4.5 \pm 0.13	<0.001
LH/CT Ratio \pm SD	1.43 \pm 0.81	0.48 \pm 0.31	<0.001	1.13 \pm 0.71	0.62 \pm 0.11	<0.001

SD: Standard deviation, L-H: Lunate-hamate distance, C-T: Capitate-triquetrum distance

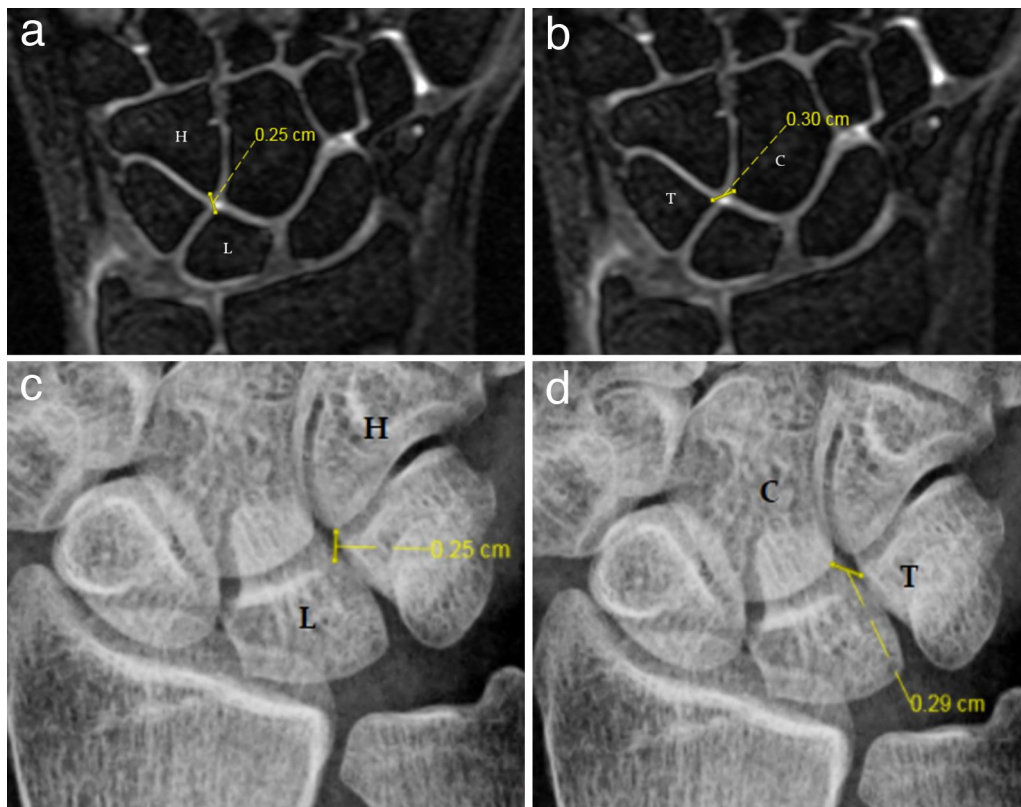


Figure 3: The measurements of lunate (L)- hamate (H) (a) and capitate (C)- triquetrum (T) distances (b) on a 3D-DESS image are shown in a patient with type 1 lunate. Radiographic measurements of lunate (L)- hamate (H) (c) and capitate (C)- triquetrum (T) distances (d) in a patient with type 1 lunate on plain radiograph are shown

Table 3: Cut-off and their respective AUC, sensitivity, specificity values for detection of type 2 lunate based on measurements of distances and their ratios between hamate- lunate and capitate- triquetrum on MRI and radiographs

		Cut-off	AUC (95% CI)	p-value	Sensitivity (%)	Specificity (%)
MRI	H-L distance (mm)	2.85 mm	0.898 (83.9-95.7)	0.03	90.9	73.3
	C-T distance (MRI) (mm)	3.4 mm	0.952 (91.6-98.9)	<0.001	92	80
	H-L/C-T ratio (MRI)	0.907	0.962 (92.9-99.5)	<0.001	95.5	83.3
X-rays	H-L distance (XR) (mm)	2.95 mm	0.713 (61.3-81.4)	0.001	67	60
	C-T distance (XR) (mm)	4.05 mm	0.801 (71.4-88.8)	<0.001	72.7	73.3
	H-L/C-T ratio (XR)	0.75	0.796 (70.8-88.5)	<0.001	75	73.3

H-L: Hamate-lunate, C-T: Capitate-triquetrum, AUC: Area under the curve, CI: Confidence interval, MRI: Magnetic resonance imaging, AUC: Area under the curve

values for H-L/C-T ratio of approximately 0.9 and 0.75 enabled better assessment of type 2 lunate with 95.5% sensitivity, 83.3% specificity and 75% sensitivity and 73.3% specificity for MRI and PA radiographs respectively.

Lunate and TFC are in the focus of the two well-known ulnar-sided painful wrist syndromes, namely hamatolunate impingement and ulnar impaction syndromes. Ulnar impaction syndrome is characterized by chronic impaction between ulnar head, TFCC, lunate and triquetrum, leading to degenerative tear of TFCC, cartilage damage on lunate, triquetrum and ulnar articular surfaces, as well as lunotriquetral ligament injury, resulting in osteoarthritis of ulnocarpal and distal radioulnar joints (14,26-28). Positive ulnar variance and dynamic changes in ulnar variance related to habitual movements and patient's occupation are well-known risk factors (29-31). Using PA radiographs, Park et al. (21) have found that ulnar impaction syndrome is more common in the wrists with a greater C-T distance and higher ulnar coverage ratio in patients with positive ulnar variance. With difference in ligamentous anatomy between the two lunate types, kinematic studies also revealed that a type 2 lunate extends later than type 1 lunate during ulnar deviation, evoking symptoms of ulnar impaction (6,9,21,32). Moreover, it was shown that lunotriquetral interosseous ligament tears were more common in type 2 lunate wrists (8,33). Thus we were surprised by the lack of an association between lunate morphology and degenerative changes in TFC. Further confirming our result, we did not observe any correlation between degenerative changes in TFC and findings of cartilage damage on proximal hamate or medial lunate facets. Our results may be partly explained by the exclusive inclusion of patient with neutral ulnar variance. In their cadaveric study, Pfirrmann et al. (8) have found twice as many TFC lesions in wrists with type 2 lunate but they concluded that due to their small sample size this difference was not statistically significant. Our study, with 118 patients supported their findings.

In this study, using a cartilage sensitive MRI sequence and defining a type 2 lunate whenever abutting articular cartilage surfaces between lunate and hamate are present, we found that

the majority of wrists (74.6%) showed a type 2 morphology, only slightly higher than the highest reported rate of 73% in an earlier study (3). Anatomical studies reveal that medial lunate facet may be as short as 1.2-2 mm (7,8).

With this definition, our aim was to correctly assess all type 2 lunates, including those with very small medial facets. The variations in reported type 1-to type 2 lunate rates in each study may be partially explained by the use of different definitions in different studies. The various methods described in anatomy and radiology literature include direct assessment of an accessory articular facet on lunate apposing hamate bone, measurement of the length of medial lunate facet, measurement of the shortest distance between the C-T distance, presence of an obvious concavity of at least 10% of lunate surface apposing hamate with a concave or a straight articular surface contiguous on at least two consecutive coronal MR images (5,7,8,17,32). All these various definitions suggest that assessing lunate type accurately is not easy. Type 2 lunates with small medial facets are not always identifiable on radiographs or even coronal computed tomography images (11,17,24). Special gradient-echo sequences, namely 2D-MEDIC and 3D-DESS images with a slice thickness of as low as 0.8 mm enabled us to evaluate the lunate - hamate relationship in their entirety.

In order to obtain more objective results, we also performed measurement based assessment of lunate types on MRI and PA radiographs. Earlier studies indicated the use of C-T distance to discriminate type 2 lunates (4,20,21,32), where ≤ 2 mm indicated a type 1 and ≥ 4 mm indicated a type 2 lunate. However, for joints with a C-T distance between 2-4 mm, the researchers defined an intermediate group in which lunate type was indeterminate (32). In their study using MR-arthrography to correlate PA radiographic findings, Park et al. (4) have reported that more than half of their study population (50.7%) was in the intermediate group. In their cadaveric study, Pfirrmann et al. (8) showed 77% occupation of the medial lunate facet and reported that the size of the medial facet is not uniform throughout consecutive coronal images on MR-arthrography. Using a distance ratio of H-L to C-T, we could observe higher sensitivity and specificity to discriminate type 2 lunates on both MRI and PA radiographs.

Yet, our results confirmed that PA radiographs had limited use in morphologic assessment of lunate, as they fail to demonstrate small medial facets (4). Moreover, the medial facet is often larger dorsally and may be completely absent on the most volar side, making the assessment even more challenging due to the 2-dimensionality of the radiographic technique (4,8). In addition to its use in assessing lunate types, the MRI threshold of 0.907 for H-L/C-T ratio was also significantly associated with hamate-sided cartilage injury in our study cohort ($p=0.01$), so this method may be useful to indicate wrists at risk for developing hamatolunate impingement.

Age was a significant factor in degeneration of all three cartilage surfaces we evaluated. Surprisingly, despite observing a close correlation between type 2 morphology and cartilage damage at the proximal pole of hamate similar to earlier researchers, we did not find such a correlation for medial lunate facet (3,5-7). Compared to hamate-sided lesions (43.2%), only 29.5% of the lunates showed chondral damage. We believe this difference could be due to our relatively younger patient cohort (mean age of 38.5 years) as most previous studies were performed on older patient populations (6,8,34).

Study Limitations

Our study has several limitations. Firstly, due to its retrospective design, we could not verify our findings with arthroscopy. However, using the dedicated cartilage sequences which have a high sensitivity and specificity for detection of cartilage lesions, we believe we could make adequate assessments.

Secondly, in order to maximize the accuracy of our findings, we only included lesions of TFC, however other components of TFCC require further studies to be evaluated, preferably using MR-arthrography.

Lastly, by including patients with neutral ulnar variance, and only assessing the PA radiographs we could not test our cut-off values on patients who have positive or negative ulnar variance or correlate our findings on other radiographic projections.

Conclusion

In conclusion, no significant association was found between lunate morphology and degenerative lesions of TFC however, age was significantly associated with degenerative changes of all cartilage surfaces. On 3D gradient-echo images direct abutment of lunate and hamate chondral surfaces may be easily detected which would indicate the presence of a type 2 morphology. When dedicated cartilage-specific MRI sequences are not available, H-L/C-T distance ratios of 0.907 on coronal MR images and 0.75 on PA radiographs could be used to better assess true type 2 lunate morphology.

Ethics

Ethics Committee Approval: Ethics committee approval was obtained for the study by Ankara University Faculty of Medicine Ethics Committee (Approval no: 10-789-19, Date: 27.05.2019).

Informed Consent: Patient informed consent was waived.

Peer-reviewed: Externally peer-reviewed.

Authorship Contributions

Surgical and Medical Practices: Concept: Design: Data Collection and Processing: Analysis or Interpretation: Literature Search: Writing: All authors have contributed equally.

Conflict of Interest: The authors declared no conflicts of interest with respect to the authorship and/or publication of this article.

Financial Disclosure: The authors received no financial support for the research and/or authorship of this article.

References

- Patterson RM, Nicodemus CL, Viegas SF, et al. High-speed, three-dimensional kinematic analysis of the normal wrist. *J Hand Surg Am.* 1998;23:446-453.
- Viegas SF. The lunatohamate articulation of the midcarpal joint. *Arthroscopy.* 1990;6:5-10.
- Viegas SF, Patterson RM, Hokanson JA, et al. Wrist anatomy: Incidence, distribution, and correlation of anatomic variations, tears, and arthrosis. *J Hand Surg Am.* 1993;18:463-475.
- Park JH, Kang TW, Choi J, et al. Radiographic prediction of lunate morphology in Asians using plain radiographic and capitate-triquetrum distance analyses: Reliability and compatibility with magnetic resonance arthrography (MRA) findings. *BMC Musculoskelet Disord.* 2019;20.
- Viegas SF, Wagner K, Patterson R, et al. Medial (hamate) facet of the lunate. *J Hand Surg Am.* 1990;15:564-571.
- Nakamura K, Patterson RM, Moritomo H, et al. Type I versus type II lunates: Ligament anatomy and presence of arthrosis. *J Hand Surg Am.* 2001;26:428-436.
- Malik AM, Schweitzer ME, Culp RW, et al. MR imaging of the type II lunate bone: Frequency, extent, and associated findings. *AJR Am J Roentgenol.* 1999;173:335-338.
- Pfirrmann CWA, Theumann NH, Chung CB, et al. The hamatolunate facet: Characterization and association with cartilage lesions - Magnetic resonance arthrography and anatomic correlation in cadaveric wrists. *Skeletal Radiol.* 2002;31:451-456.
- Bain GI, Clitherow HDS, Millar S, et al. The effect of lunate morphology on the 3-dimensional kinematics of the carpus. *J Hand Surg Am.* 2015;40:81-89.e1.
- Nakamura K, Beppu M, Patterson RM, et al. Motion analysis in two dimensions of radial-ulnar deviation of type I versus type II lunates. *J Hand Surg Am.* 2000;25:877-888.
- Nakamura K, Beppu M, Matsushita K, et al. Biomechanical Analysis of the Stress Force on Midcarpal Joint in Kienb \ o ck's Disease. *Hand Surgery.* 1997;02:101-115.
- Thurston AJ, Stanley JK. Hamato-lunate impingement: An uncommon cause of ulnar-sided wrist pain. *Arthroscopy.* 2000;16:540-544.
- Watanabe A, Souza F, Vezeridis PS, et al. Ulnar-sided wrist pain. II. Clinical imaging and treatment. 2010. pp. 837-857.
- Cerezal La. Imaging findings in ulnar-sided wrist impaction syndromes. *Radiographics.* 2002;22:105-121.

15. Radiographic analysis of anatomical risk factors for Kienböck's disease. *Acta Orthop Belg.* 2004;70:406-409.
16. Rhee PC, Jones DB, Moran SL, et al. The effect of lunate morphology in Kienböck disease. *Journal of Hand Surgery.* 2015;40:738-744.
17. McLean JM, Turner PC, Bain GI, et al. An association between lunate morphology and scaphoid-trapezium-trapezoid arthritis. *Journal of Hand Surgery: European Volume.* 2009;34:778-782.
18. Hein RE, Fletcher AN, Tillis RT, et al. Association of Lunate Morphology With Progression to Scaphoid Fracture Nonunion. *Hand.* 2020;17:452-458.
19. Rhee PC, Moran SL, Shin AY. Association Between Lunate Morphology and Carpal Collapse in Cases of Scapholunate Dissociation. *Journal of Hand Surgery.* 2009;34:1633-1639.
20. Kim BJ, Kovacevic D, Lee YM, et al. The role of lunate morphology on scapholunate instability and fracture location in patients treated for scaphoid nonunion. *CiOS Clinics in Orthopedic Surgery.* 2016;8:175-180.
21. Park JH, Jang WY, Kwak DH, et al. Lunate morphology as a risk factor of idiopathic ulnar impaction syndrome. *Bone Joint J.* 2017;99B:1508-1514.
22. Saupé N. 3-Tesla high-resolution MR imaging of the wrist. *Semin Musculoskelet Radiol.* 2009;13:29-38.
23. Yoshioka H, Burns JE. Magnetic resonance imaging of triangular fibrocartilage. *J Magn Reson Imaging.* 2012;35:764-778.
24. Sagerman SD, Hauck RM, Palmer AK. Lunate morphology: Can it be predicted with routine x-ray films. *J Hand Surg Am.* 1995;20:38-41.
25. Oneson SR, Scales LM, Timins ME, et al. MR imaging interpretation of the Palmer classification of triangular fibrocartilage complex lesions. *Radiographics.* 1996;16:97-106.
26. Escobedo EM, Bergman AG, Hunter JC. MR imaging of ulnar impaction. *Skeletal Radiol.* 1995;24:85-90.
27. Friedman SL, Palmer AK. The ulnar impaction syndrome. *Hand Clin.* 1991;7:295-310.
28. Sammer DM, Rizzo M. Ulnar impaction. *Hand Clin.* 2010;26:549-557.
29. Palmer AK, Glisson RR, Werner FW. Ulnar variance determination. *J Hand Surg Am.* 1982;7:376-379.
30. Palmer AK, Glisson RR, Werner FW. Relationship between ulnar variance and triangular fibrocartilage complex thickness. *J Hand Surg Am.* 1984;9:681-683.
31. Tomaino MM. The importance of the pronated grip x-ray view in evaluating ulnar variance. *J Hand Surg Am.* 2000;25:352-357.
32. Galley I, Bain GI, McLean JM. Influence of Lunate Type on Scaphoid Kinematics. *J Hand Surg Am.* 2007;32:842-847.
33. Harley BJ, Werner FW, Boles SD, et al. Arthroscopic resection of arthrosis of the proximal hamate: A clinical and biomechanical study. *J Hand Surg Am.* 2004;29:661-667.
34. McLean JM, Bain GI, Watts AC, et al. Imaging Recognition of Morphological Variants at the Midcarpal Joint. *J Hand Surg Am.* 2009;34:1044-1055.